Design and Optimization of Comb Drive Accelerator for High Frequency Oscillation

Zichen Zhang

Abstract

Comb-drive devises have been widely applied in many fields. However, the application of high frequency sensor, such as rocket chamber, still remains problems. In this work, a finite element code was used for the design, optimization and visualization of a comb drive accelerator. In the simulation results, the post-optimization design has high performance in high frequency oscillation operating environment. The optimization is based on the ideal eigen frequency and Nelder-Mead method. The 3-D working conditions are realized by testing and comparing the time and frequency domain of pre-optimized and optimized design which frequency ranges from 2000 Hz to 5000 Hz. Finally, the electric potential and capacitance in comb drive is visualized, which shows the better electric signals and displacements.

Key Words: comb drive, design, optimization, 3-D simulation, COMSOL, frequency.

Introduction

In contemporary society, the Micro-Electro-Mechanical System (MEMS) devices have played a significant role in many fields, e.g. accelerator, fluid control, micro-power system, MEMS fuse system and internet of things (IOT)[1]. The widely use of MEMS devices is due to its scaling advantage, i.e. the scaling of MEMS devices reduces the cost per device. Although the total cost to fabricate one wafer may increase, the number of devices on each wafer increases exponentially with the decrease of the feature size of MEMS devices. In addition, the finer fabrication process provides high performance of MEMS devices. For example, the accuracy and precision of MEMS sensors are orders of magnitude higher than conventional sensors. [2] Therefore, MEMS has become a focus of both fundamental research and applicable engineering. Among all the MEMS applications, the comb drive uses electrostatic force as the actuation principle. There are two metal conductors in the micro-scale shape of the comb. They both alternate with each other where one is static and the other is dynamic.

When passing an alternating current, one of the comb will be moving which relative to another conductor. More specifically, more and more scientists prefer to use the comb drives for electrostatic actuation, capacitive position sensing and frequency turning.[3] They have become an inalienable part of many MEMS devices such as accelerometers, gyroscopes, and micro scanners and so forth.[4] The rocket combusting chamber has a specific vibrating frequency, which is usually within the range between 1000 to 5000 Hz. The design and development of a micro-accelerator becomes an essential problem for real-time monitor of the working stators of the combusting chamber.

However, the design and optimization of comb drive sensor becomes a challenge for the society since the geometry of the devices is complex. Xie et al has already designed and fabricated the out of plane comb drives which can achieve the aim of realizing.[5] Based on Xie's design, some scientists have already successfully developed and tested 1-D analog scanning micro mirror arrays with hidden vertical comb-drive actuators.[6] Besides, there are also some other groups using comb drive to solve out sophisticated problems as to overcome the difficulties of isolating two stationary capacitor comb sets in bulk micromachining by the electrically.[7] Whereas, those designs lack of the freedom to change all the parameters of the comb drive, which means that the designs are partially fixed. Moreover, there is no visualization in their models, making it hard to show the results of the model.

In this work, I used the powerful simulation software---COMSOL to make the model more vivid and visual. The study of the vertical comb-finger actuation for CMOS MEMS is also been realized, simulated and tested. In addition, behavioral simulation using the 3-D NODAS library matches the experimental results within 7% for frequency response.[8] Comparing with this work, the frequency domain study was conducted to optimize the model which nobody has involved in this filed. I also parameterized the geometry of the comb drive structure, e.g. fingers and stators. As a result, I can easily change the structure for optimization in the model. In this way, the model can solve the problems that have mentioned above.
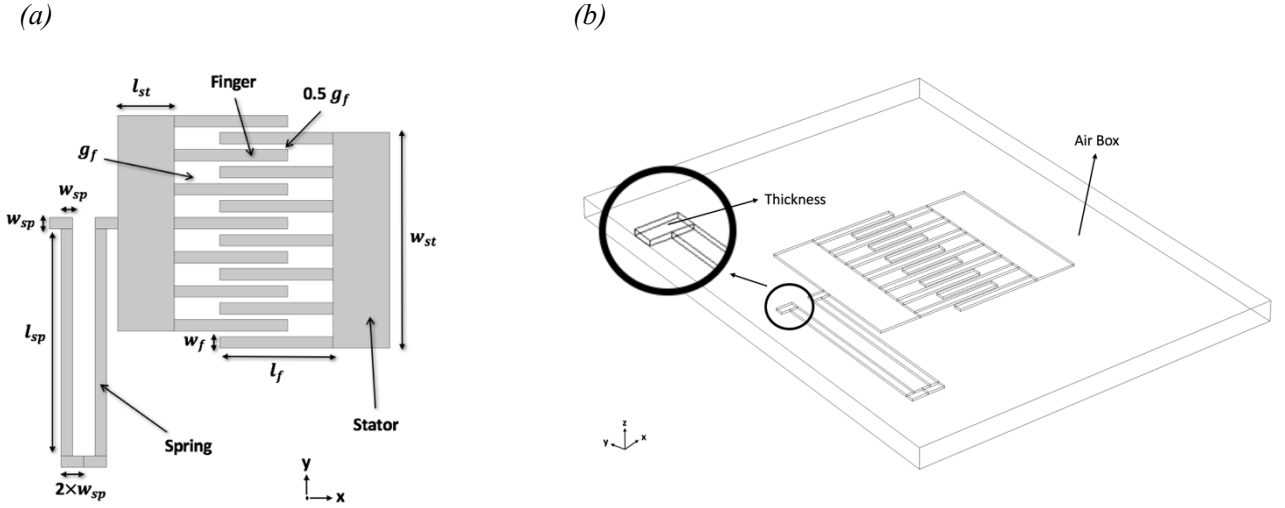
Model setup

Fig.1 (a) 2-D plane schematic of the comb drive

(b) 3-D stereoscopic schematic of the comb drive

The schematic of the comb drive used in this work is shown in Fig.1, in which (a) and (b) shows the plane and the stereoscopic geometry respectively. Parameterization makes it easy to change the specific numerical number of different parts. In Fig. 1(a), the comb drive has five fingers in both the static (right) and moving (left) combs. To better describe the structure, I use w to represent the width of stators (st), fingers (f) or spring (sp), l to represents the length, and g for gaps between two fingers. In order to stimulate the real working circumstance of comb drives, Fig. 1(b) shows the ***thickness*** of structures, and the ***air box*** as the air around the comb drive in three dimension. The airbox is setup to calculate the electric field in the air. In order to adapt the rocket chamber circumstances, the number of fingers is fixed as five, the material is copper, and environment is 293.15K for temperature, 1 atm for absolute pressure which have been all set up in COMSOL.

Before the optimization, each parameter is set up the proper number, as 200μm for l_f, w_f 20μm , l_{st} 100μm, g_f 20μm, l_{sp} 400μm, w_{sp} 20 μm, and w_{st} expresses as:

$$w_{st} = 6w_f + 5(g_f + w_f) \tag{1}$$

which can derive that w_{st} is 380μm. On the other hand, the thickness is 5μm, and the size of **air box** is large enough to cover the whole model.

After fixing the right stator, I apply an oscillating voltage with 1V amplitude to the left comb. The relation between the displacement, u, and the time domain, t, which is the first 1 ms, can be easily obtained by solving the equation below:

$$\rho \ddot{u} = \nabla \cdot s + F_V \tag{2}$$

where ρ is the density, s is the stress tensor and Fv is the external force density.

Fig. 2 shows the displacement of the moving comb after applying an oscillating voltage at the comb drive by applying 1 V.
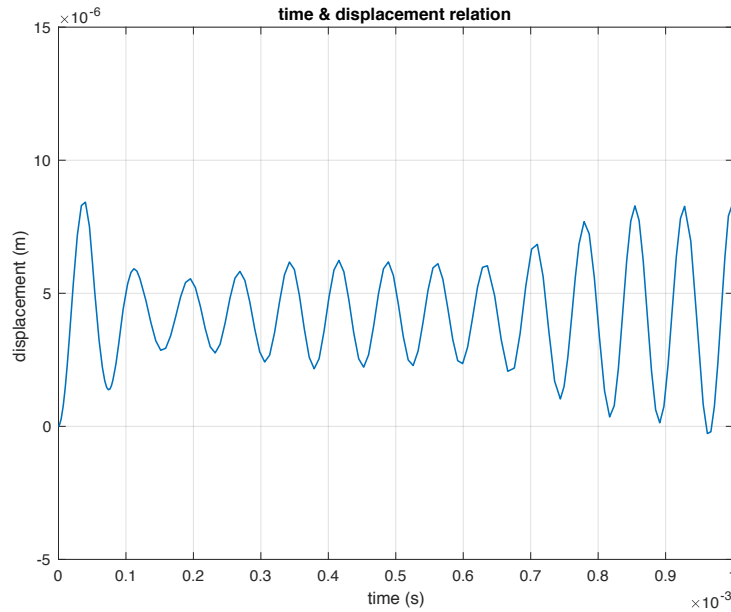
Fig 2. the initial relation between displacement and the time

Then we simulate the deformation of the moving comb in the frequency domain. The frequency ranges from 2000 Hz to 5000 Hz, which is the average frequency of the rocket, is used to calculate the

displacement, **u.** The inertia force applied on the moving comb is set to be constant. We expect the larger displacement with the same inertia force amplitude since the larger displacement can induce more significant electric signal change. Thus, we can optimize the structure in order to obtain the maximum displacement in the frequency where the rocket chamber operates. In the end, we compare this pre-optimized design (**PD**) to with the optimized design (**OD**) to show the improvement of the device.

Different displacement fields with different frequencies (**freq**) are shown in Fig.3 (a) to (d). The volume color represents the displacement field for each parts.
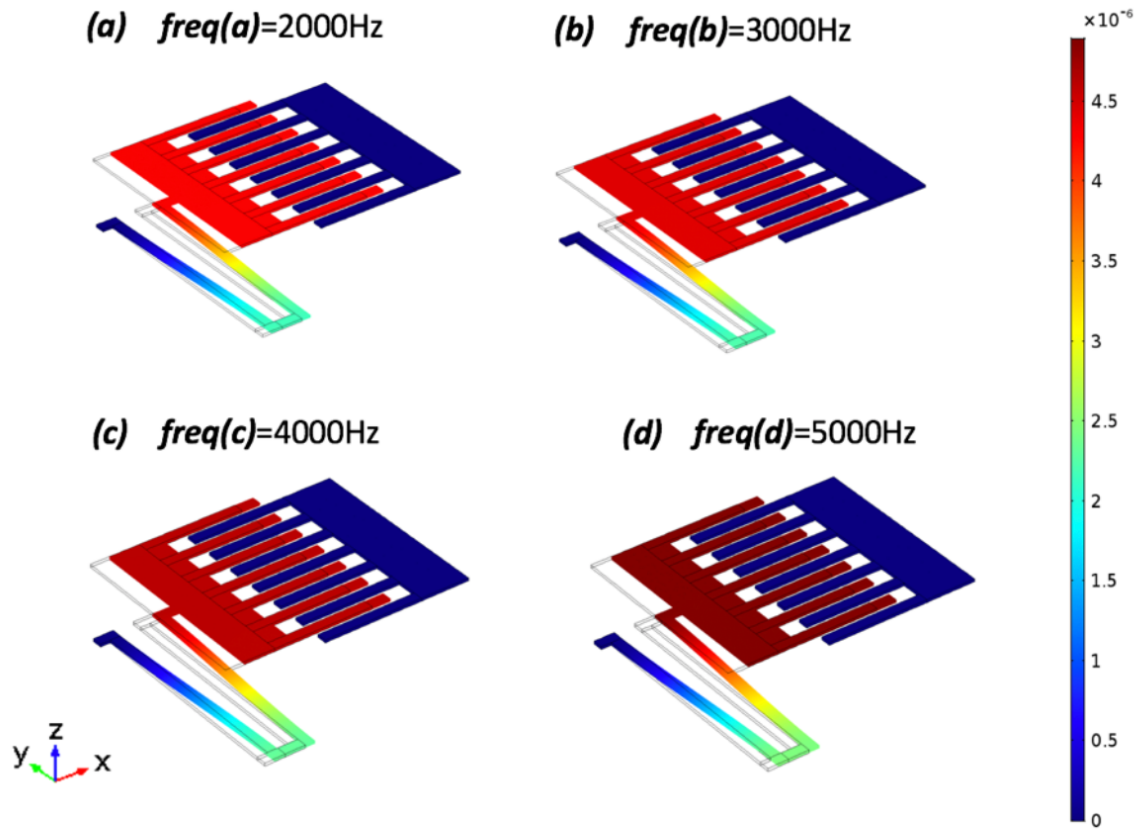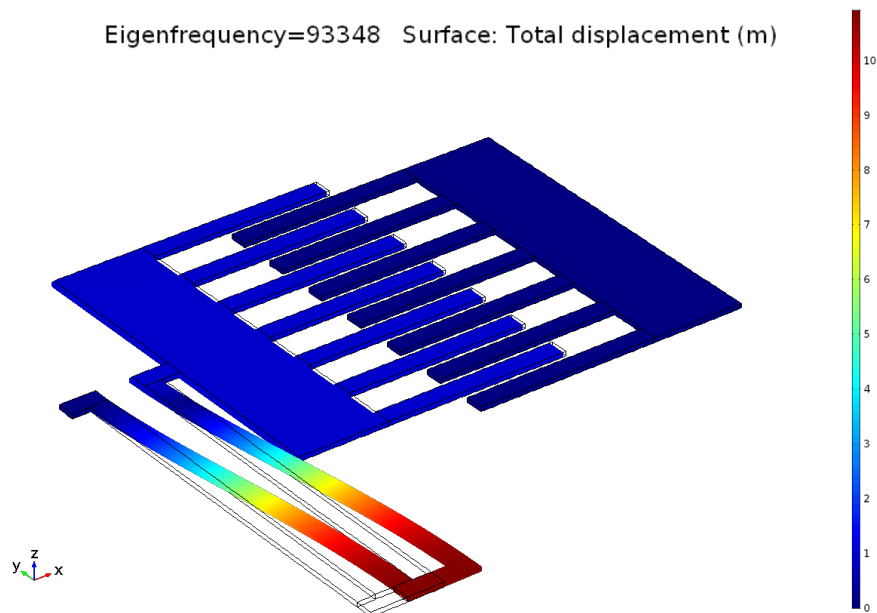

Fig.3 (a), (b), (c), (d), reflect the visualized displacement by colors when frequency is 2000Hz, 3000Hz, 4000Hz and 5000Hz respectively.

Result

First, the eigen modes of the mechanics are evaluated. As widely known, the rocket chamber operating frequency has a range from 5000 – 10000 Hz, which is our objective frequency. The eigen frequency should be as close as the objective to output the maximum displacement. For the physical material, the specific frequency which reach the maximum amplitude is called Eigen frequency. Before the optimization, the eigen frequencies of the pre-optimized design's (**PD**) are far away from 5000Hz which is the operation frequency of the rocket chamber. As a result of the frequency mismatch, the performance of the PD is not considered appropriate for the rocket chamber application. Fig.5 shows two the eigen modes of device. The color in Fig.5 represent the displacement field of the drive.

(a)

Eigenfrequency=93348 Surface: Total displacement (m)

(b)

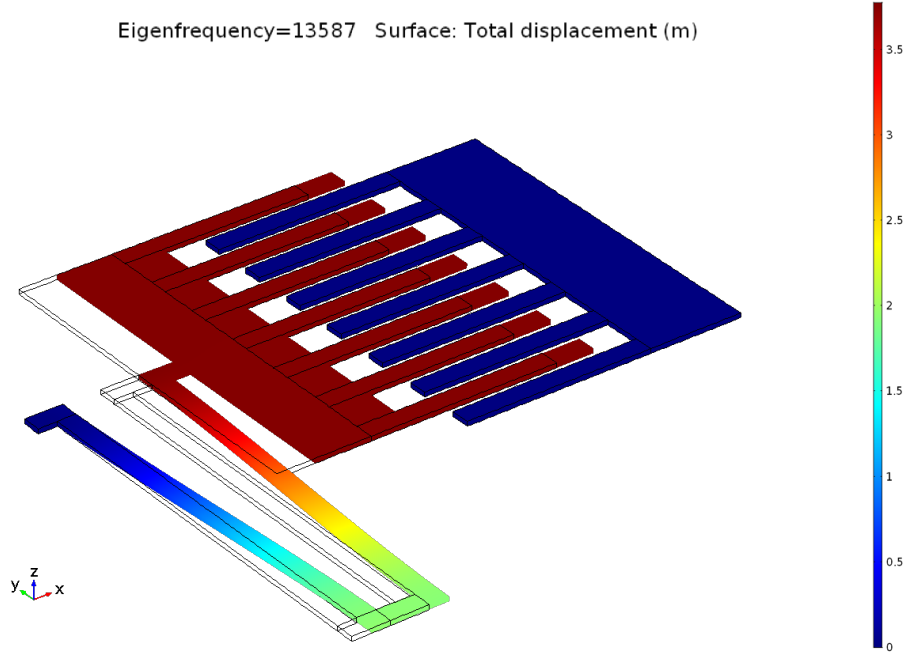Eigenfrequency=13587   Surface: Total displacement (m)

Fig.4 (a), (b) show two different working performance of two Eigen frequency around 10000 Hz.

To compare these two different modes, the second eigen mode (Fig 5.b) has translational motion of the left comb with 13587Hz. It should be mentioned that we expect the translational mode rather than other modes. In translational mode, all the left fingers move toward the stator coherently.

The optimization used Nelder-Mead method to obtain the better performance of the comb drive accelerator. The variable in the optimization is the length of the suspension spring l_f . The constraint boundary of l_f is set up to vary from 180 μm to 200 μm, while l_s varies from 80 μm to 120 μm. The goal of the optimization is to get the frequency of the translational mode to as close as 10000 Hz. Therefore, the objective of the optimization is the square of the difference between the translational mode frequency and the designated 10000 Hz. The math is to minimize this objective while using different geometries of the comb drive. Represented results of the optimization are shown in *Table 1*.

Table 1

The optimization results

l_finger (m)	l_stator (m)	Objective
$2.00×10^{-4}$	$1.00×10^{-4}$	$1.2869×10^7$
$1.98×10^{-4}$	$1.00×10^{-4}$	$1.3063×10^7$
$2.00×10^{-4}$	$1.02×10^{-4}$	$1.2370×10^7$
$1.96×10^{-4}$	$1.00×10^{-4}$	$1.3250×10^7$
$2.00×10^{-4}$	$9.80×10^{-5}$	$1.3389×10^7$
$2.00×10^{-4}$	$1.20×10^{-4}$	$8.5970×10^6$

It can be found that, when l_f equals to 2 µm with 1.2 µm l_s, the Eigen frequency is closest to the

10000Hz where our design goal is achieved.

After adapting all the parameters from the optimization, we built the optimized design (**OD**) and

tested the new design to compared its performance with our original design. Comparison of the

displacement is shown in T*able 2*. Fig.6 shows the difference performance between **PD** and **OD** in the

frequency range of the rocket chamber.

Table 2

The relation between frequency and displacement of PD and OD

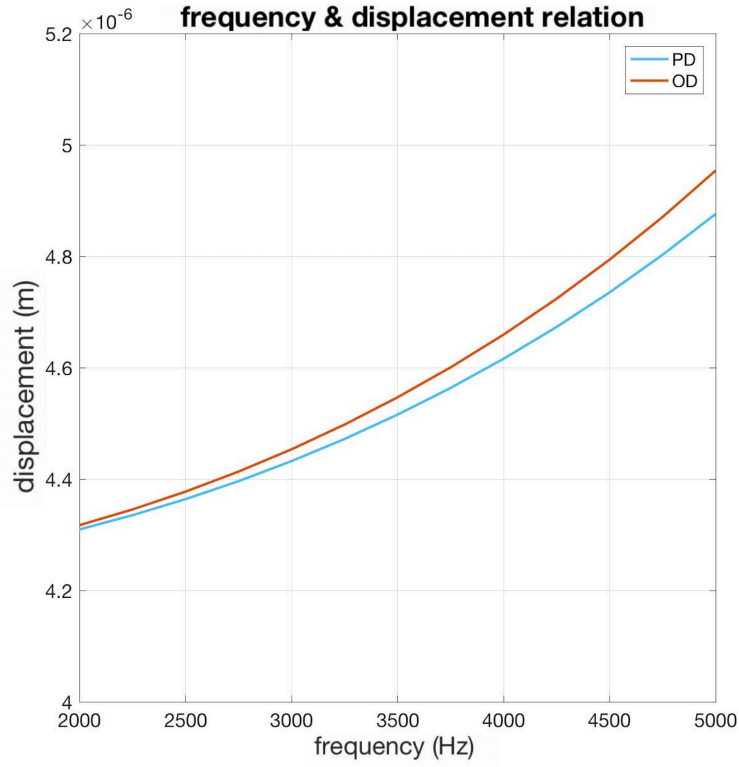| Frequency (Hz)	PD Displacement (m)	OD Displacement (m)
2000	$4.3095×10^{-6}$	$4.3171×10^{-6}$
2250	$4.3350×10^{-6}$	$4.3453×10^{-6}$
2500	$4.3638×10^{-6}$	$4.3773×10^{-6}$
2750	$4.3961×10^{-6}$	$4.4133×10^{-6}$
3000	$4.4321×10^{-6}$	$4.4533×10^{-6}$
3250	$4.4718×10^{-6}$	$4.4977×10^{-6}$
3500	$4.5156×10^{-6}$	$4.5467×10^{-6}$
3750	$4.5635×10^{-6}$	$4.6004×10^{-6}$
4000	$4.6159×10^{-6}$	$4.6593×10^{-6}$
4250	$4.6730×10^{-6}$	$4.7237×10^{-6}$
4500	$4.7351×10^{-6}$	$4.7939×10^{-6}$
4750	$4.8027×10^{-6}$	$4.8705×10^{-6}$
5000	$4.8759×10^{-6}$	$4.9539×10^{-6}$

Fig. 5 Relation between Frequency and Displacement of PD and OD.

Next, we simulated the relation between the applied forces and displacements. The results of frequency dependent displacement are presented in *Table 3*. By applying the same force, the OD has significantly larger displacement than that of PD. Thus, the simple test proves the displacement has ascended after optimization. Even only a small increase in the displacement, it will increase the electric signal on the micro level.

Table 3

The difference between the displacement before and after the optimization.

Applied Force	Displacement field PD	Displacement field OD	Difference
0	0	0	0
1.00	0.04216233	0.042133753	2.85769×10^5
2.00	0.08432466	0.084267506	5.71538×10^5
3.00	0.12648699	0.126401259	8.57307×10^5
4.00	0.16864932	0.168535012	1.14308×10^4
5.00	0.21081165	0.210668766	1.42885×10^4
6.00	0.25297398	0.252802519	1.71461×10^4
7.00	0.29513631	0.294936272	2.00038×10^4
8.00	0.33729864	0.337070025	2.28615×10^4
9.00	0.37946097	0.379203778	2.57192×10^4
10.00	0.42162330	0.421337531	2.85769×10^4

In the static electric domain, the electric field **E** satisfies the following relation

$$\mathbf{E} = -\nabla V \tag{5}$$

$$\nabla \cdot (\varepsilon_0 \varepsilon_r E) = \rho_v \tag{6}$$

where V is the electric potential, ε is the permittivity and ρ_v is the electric charge density. The capacitance of the device can be calculated as $C = Q/V = 3.2581 \times 10^{-14}$ F, if the device is in static.
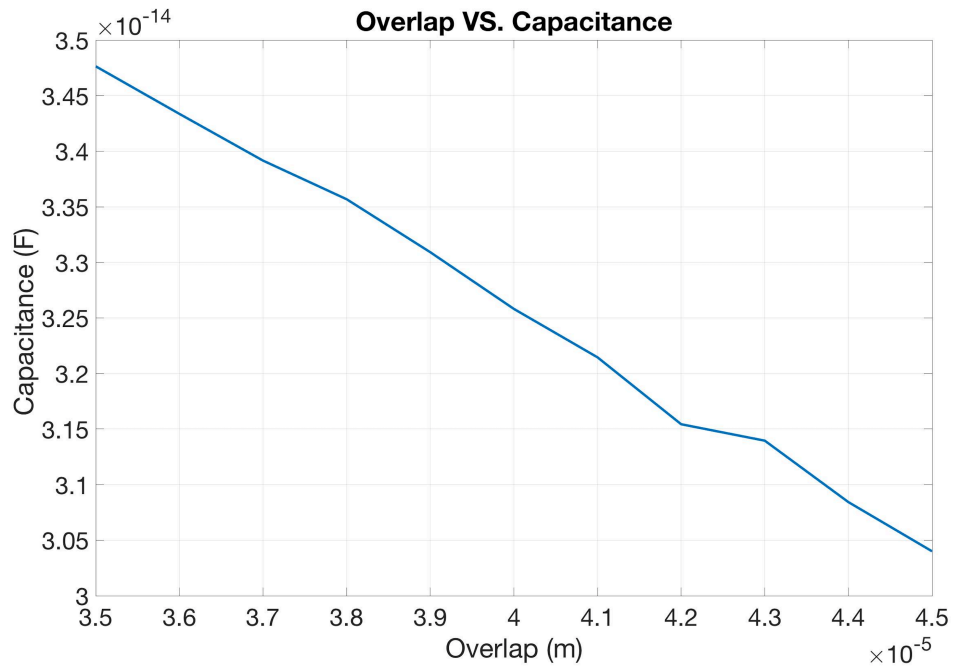
Fig. 6 Overlap versus Capacitance

Fig.6 shows the capacitance versus the length of the overlap which is induced by the external force. The capacitance can be simply estimated with the equation

$$C = \frac{\varepsilon S}{d} \tag{7}$$

where S is the effective area, and d is the effective distance between two capacitor plates. Fig. 6 indicates that as overlap grows, the capacitance of the comb drive will decrease. The change of capacitance can be easily measured by the voltage of the comb drive. This is how we interpreter the vibration in mechanics to electric signal.
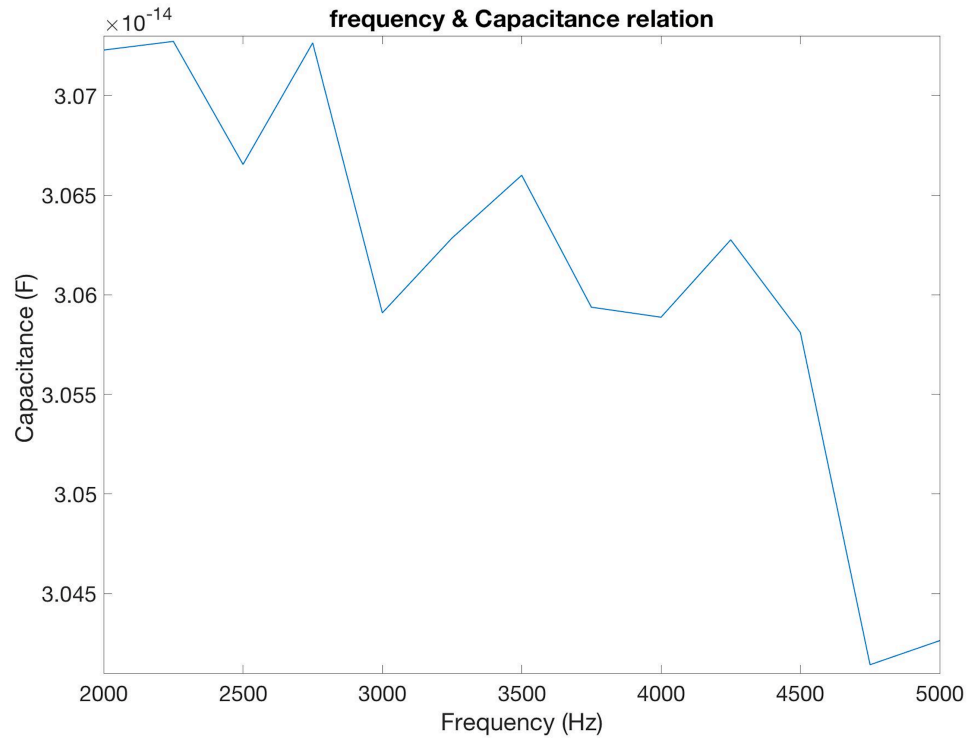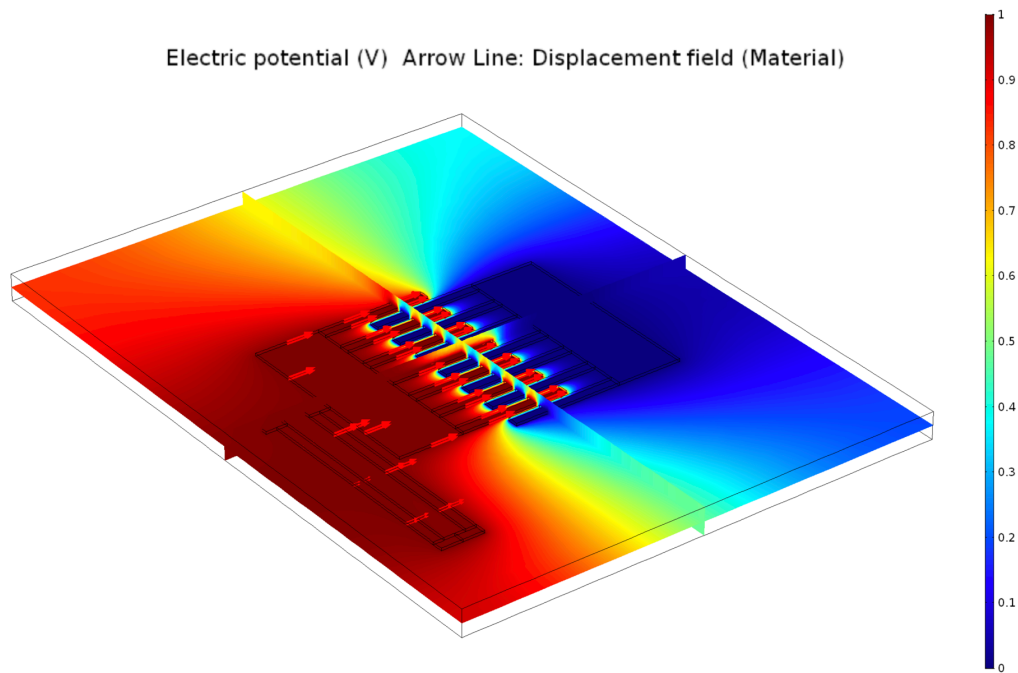
Fig.7 The Capacitances at different frequencies ranged from 2000 Hz to 5000 Hz

After applying a 10^{-3} N force to the device, it makes the displacements at frequencies ranged from 2000 Hz to 5000 Hz. If applying these displacements as the change of the overlap distance, the capacitance can be modified, which was showed the relation in *Fig.7*.

Fig. 8 (a) and (b) shows the electric equilibrium state of the deformed comb drive applied with 1V voltage. The arrows represent the electric field and the color represents the electric potential. As the movement of the device is to the right, the displacement field is positive. This figure is clear to show the distribution of the electric field in the comb drive device.

(a) the electric potential in the whole device

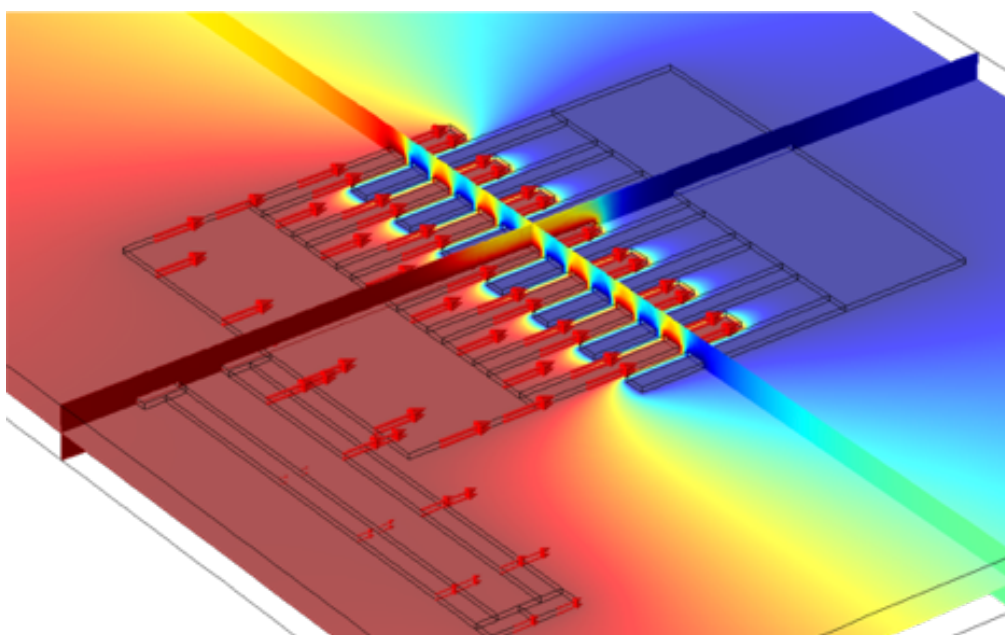*(b) The electric potential in a part of the device*

Fig. 8 (a) and (b) show the electric field potential in this device

Conclusion

In this work, comb drive devices in rocket camber is designed, optimized, simulated and tested with a fully coupled FEA model. The model realized the visualization to help the design and optimization. The OD performs order of magnitude higher sensitive in the frequency range of the working rocket chamber. The parameterization helps to change the variables quickly in this model and makes it convenient for the optimization. After the optimization, the electric filed response has been tested and by comparing with the PD model and OD model. The PD has larger electric signal in response to the mechanical vibration.

Acknowledgement

References

1. Wiak, S., Smółka, K., Dems, M. & Komęza, K. Numerical modeling of 3D intelligent comb drive accelerometer structure: Mechanical models. *COMPEL-The Int. J. Comput. Math. Electr. Electron. Eng.* **25,** 697–704 (2006).

2. Hirano, T. *et al.* Design, fabrication, and operation of submicron gap comb-drive microactuators. *J. Microelectromechanical Syst.* **1,** 52–59 (1992).

3. Xie, H., Erdmann, L., Jing, Q. & Fedder, G. K. Simulation and characterization of a CMOS z-axis microactuator with electrostatic comb drives. (2000).

4. Xie, H. & Fedder, G. K. Vertical comb-finger capacitive actuation and sensing for CMOS-MEMS. *Sensors Actuators, A Phys.* **95,** 212–221 (2002).

5. Xie, H. & Fedder, G. K. A CMOS z-axis capacitive accelerometer with comb-finger sensing. in *Micro Electro Mechanical Systems, 2000. MEMS 2000. The Thirteenth Annual International Conference on* 496–501 (IEEE, 2000).

6. Hah, D., Huang, S. T. Y., Tsai, J. C., Toshiyoshi, H. & Wu, M. C. Low-voltage, large-scan angle MEMS analog micromirror arrays with hidden vertical comb-drive actuators. *J. Microelectromechanical Syst.* **13,** 279–289 (2004).

7. Sun, Y., Fry, S. N., Potasek, D. P., Bell, D. J. & Nelson, B. J. Characterizing fruit fly flight behavior using a microforce sensor with a new comb-drive configuration. *J. Microelectromechanical Syst.* **14,** 4–11 (2005).